Numerical experiments on radiative cooling and collapse in plasma focus operated in krypton

S LEE[1,2*], S H SAW[1,2] and JALIL ALI[3]

[1]INTI International University, 71800 Nilai, Malaysia
[2]Institute for Plasma Focus Studies, 32 Oakpark Drive Chadstone, Australia
[3]Institute of Advanced Photonic Science, Nanotechnology Research Alliance, Universiti Teknologi Malaysia, 81310 Johor Baru , Malaysia

e-mails: sorheoh.saw@newinti.edu.my leesing@optusnet.com.au djxxx_1@yahoo.com

Abstract

The Plasma Focus has wide-ranging applications due to its intense radiation of SXR, XR, electron and ion beams and fusion neutrons when operated in deuterium. The 5-phase Lee Model code has been developed for the focus operated in various gases including D, D-T, He, Ne, N, O, Ar, Kr and Xe. Radiation-coupled motion is included in the modelling. In this paper we look at the effect of radiation cooling and radiation collapse in Krypton. The Pease-Braginskii current is that current flowing in a hydrogen pinch which is just large enough for the Bremsstrahlung to balance Joule heating. This radiation-cooled threshold current for a hydrogen pinch is 1.6MA. It is known that in gases undergoing line radiation strongly the radiation-cooled threshold current is considerably lowered. We show that the equations of the Lee Model code may be used to compute this lowering. The code also shows the effect of radiation cooling leading to radiative collapse. Numerical experiments are run to demonstrate a regime in which radiation collapse is observed in Kr.

PACS 52.50.Lp - Plasma production and heating by shock waves and compression
PACS 52.58.Lq - Z-pinches, plasma focus, and other pinch devices
PACS 52.59.Hq - Dense plasma focus
PACS 52.55.Dy - General theory and basic studies of plasma lifetime, particle and heat loss, energy balance, field structure, etc.

1. Introduction

The Plasma Focus has wide-ranging applications due to its intense radiation of SXR, XR, electron and ion beams, and fusion neutrons [1] when operated in Deuterium. The use of gases such as Ne and Xe for generation of specific SXR or EUV lines for micro-lithography applications [2] has been widely discussed in the literature as has the use of N and O to generate the lines suitable for water-window microscopy [3]. Recently Ar has been considered for micro-machining due to the harder characteristic line radiation [4]. Various gases including Kr have been discussed and used for fusion neutron yield enhancement [5] due arguably to mechanisms such as thermodynamically enhanced pinch compressions. Not so often mentioned is the possibility of intense radiation leading to extreme compressions and the implications of such a mechanism for development of radiation sources. In this paper we look at the effect of radiation cooling and radiation collapse in the Krypton. The Pease-Braginskii current [6,7] is known to be that current flowing in a hydrogen pinch which is just large enough for the Bremsstrahlung to balance Joule heating. This radiation-cooled threshold current for a hydrogen pinch is 1.6MA. It is known that in gases undergoing line radiation strongly the radiation-cooled threshold current is considerably lowered [8]. We show that the equations of the Lee Model code [9] may be used to

compute this lowering. It is suggested that the neutron enhancement effect of seeding could at least in part be due to the enhanced compression caused by radiation cooling.

We discuss here the 5-phase Lee Model code for the focus operated in Kr. A corona model is used to generate the thermodynamic data required in the computation.

2. The Lee model code

The Lee model code couples the electrical circuit with plasma focus dynamics, thermodynamics, and radiation, enabling a realistic simulation of gross focus properties. The basic model [10] was successfully used for several projects [11-14]. Radiation-coupled dynamics was included, leading to numerical experiments on radiation cooling [15]. The vital role of a finite small disturbance speed [16] was incorporated together with real gas thermodynamics and radiation-yield terms. This version assisted other projects [17-21] and was web published [22] with plasma self-absorption included in 2007 [22], improving the SXR yield simulation. The code has been used in several machines including UNU/ICTP PFF [2,13-15,18-21], NX2 [2,4,17,23], and NX1[2] and has been adapted for the Filippov-type plasma focus DENA [24]. A recent development includes neutron yield Y_n using a beam–target mechanism [25-29], incorporated in recent versions [9] of the code (after RADPFV5.13), resulting in realistic Y_n scaling with I_{pinch} [30-32]. The versatility of the model is demonstrated in its distinction of I_{pinch} from I_{peak} [27] and the recent uncovering of a pinch current limitation effect [28,29], as static inductance is reduced towards zero. Numerical experiments uncovered neutron [25,26,30] and SXR [33-36] scaling laws over a wider range of energies and currents than attempted before and gave insight into the nature and cause of 'neutron saturation' [30].

A brief description of the 5-phase model is given in the following.

2.1 The 5 phases

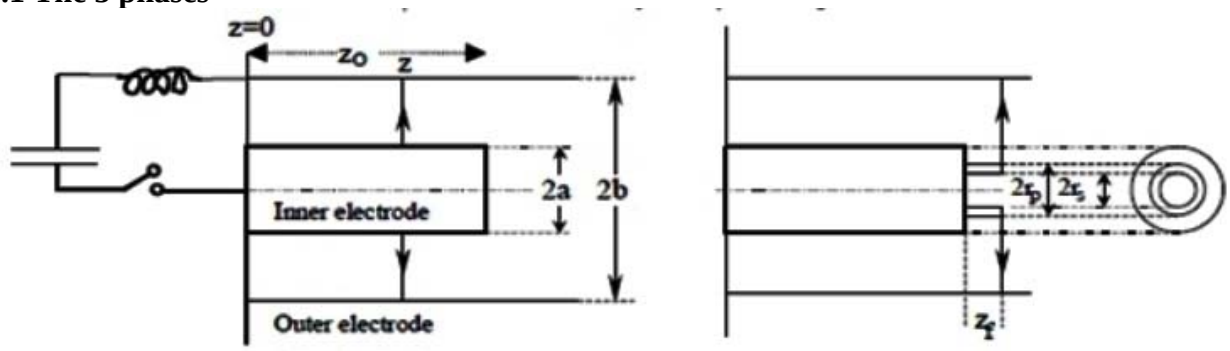

Figure 1. Schematic of the axial and radial phases. The left section depicts the axial phase, the right section the radial phase. In the left section, z is the effective position of the current sheath-shock front structure. In the right section r_s is the position of the inward moving shock front driven by the piston at position r_p. Between r_s and r_p is the radially imploding slug, elongating with a length z_f. The capacitor, static inductance and switch powering the plasma focus is shown for the axial phase schematic only.

The five phases (*a*-*e*) are summarised [9,36] as follows:

a. Axial Phase (see Figure 1 left part): Described by a snowplow model with an equation of motion which is coupled to a circuit equation. The equation of motion incorporates the axial phase model parameters: mass and current factors f_m and f_c. The mass swept-up factor [37] f_m accounts for the porosity of the current sheet, the inclination of the current sheets-shock front structure, boundary layer and all other unspecified effects which changes the amount of mass in the moving structure. The current factor f_c accounts for the fraction of current effectively flowing in the moving structure due to all effects such as current shedding and current sheet inclination

b. Radial Inward Shock Phase (see Figure 1 right part): Described by 4 coupled equations using an elongating slug model. The first equation computes the radial inward shock speed from the driving magnetic pressure. The second computes the axial column elongation speed. The third computes the speed of the current sheath (magnetic piston), allowing the sheath to separate from the shock front [16]. The fourth is the circuit equation. Thermodynamic effects due to ionization and excitation are incorporated. Temperature and number densities are computed using shock-jump equations. The model parameters, radial phase mass swept-up and current factors f_{mr} and f_{cr} are incorporated in all three radial phases.

c. Radial Reflected Shock (RS) Phase: When the shock front hits the axis, because the plasma is collisional, a reflected shock develops which moves radially outwards, whilst the radial current sheath continues to move inwards. Four coupled equations are used, these being for the reflected shock moving radially outwards, the piston moving radially inwards, the elongation of the annular column and the circuit. The plasma temperature behind the reflected shock undergoes a jump by a factor of 2. Number densities are computed using reflected shock jump equations.

d. Slow Compression (Quiescent) or Pinch Phase: When the out-going reflected shock hits the inward moving piston, the compression enters a radiative phase. For gases such as neon, radiation emission may enhance the compression as energy loss/gain terms from Joule heating and radiation are included in the piston equation of motion. Three coupled equations are used; these being for piston radial motion, pinch column elongation and for the circuit. The duration of this slow compression (pinch) phase is set as the time of transit of small disturbances across the pinched plasma column. The gross column is considered not including the effects of localized regions of high densities and temperatures [38].

e. Expanded Column Axial Phase: To simulate the current trace beyond this point we allow the column to suddenly attain the radius of the anode, and use the expanded column inductance for further integration. This phase is not considered important as it occurs after the focus pinch.

3 Radiation Cooling and Collapse in krypton

We look at the thermodynamic processes in krypton as it is heated to high temperatures. The ionization curves of Kr are computed from the corona model [39] using ionization data [40]. From these ionization curves the effective charge Z_{eff} and the specific Heat Ratio γ of Kr are computed [41].

The Pease-Braginskii P-B current [6,7] is the value of current (1.6 MA) at which the Bremsstrahlung (considered as a loss from the plasma) equals the Joule heating of the plasma pinch column in hydrogen assuming Spitzer resistivity. When pinch current exceeds this value, the Bremsstrahlung losses exceed Joule heating and the plasma pinch begins to experience increasingly severe radiative cooling effects at progressively higher currents until radiative collapse may be observed. The P-B current only considers Bremsstrahlung, since at the high temperatures experienced in the hydrogen or deuterium pinch, the gases are fully ionized and there is no line radiation.

For gases such as neon, argon, krypton and xenon, there may still be line radiation even at the high pinch temperatures. This line radiation may considerably exceed the effect of Bremsstrahlung. In that case, the effect of radiation cooling, and eventually radiative collapse may be exacerbated; and may occur at much lower currents [42].

3.1 Power balance

We consider the following powers (all quantities in SI units unless otherwise stated): respectively Joule heating, Bremsstrahlung and Line radiation generated in a plasma column of radius r_p, length l at temperature T:

$$\frac{dQ_J}{dt} = C_J T^{-3/2} \frac{l}{\pi r_p^2} Z_{eff}\ I^2 \quad \text{where } C_J \cong 1300 \text{ and } T \text{ is in Kelvin} \tag{1}$$

$$\frac{dQ_{Brem}}{dt} = C_1\ T^{1/2} n_i^2\ Z_{eff}^3 \pi r_p^2\ l \quad \text{where } n_i \text{ is in m}^{-3} \text{ and } C_1 = 1.6 \times 10^{-40} \tag{2}$$

$$\frac{dQ_{line}}{dt} = C_2 T^{-1} n_i^2\ Z_n^4 Z_{eff} \pi r_p^2\ l \quad \text{where } C_2 = 4.6 \times 10^{-31} \tag{3}$$

We use the Bennett distribution to obtain a relationship between T (pinch temperature) and I (pinch current) as follows:

$$T = b \frac{I^2}{(n_i r_p^2)(1 + Z_{eff})} \qquad \text{where} \quad b = \frac{\mu}{8\pi^2 k} \tag{4}$$

So that we write the total power adding the three terms as follows:

$$\frac{dQ}{dt} = -\pi \left[C_1 b^{1/2}\right] \frac{Z_{eff}^3}{(1 + Z_{eff})^{1/2}} n_i^{3/2} r_p l\ I - \frac{\pi C_2}{b} (1 + Z_{eff})\, Z_{eff} Z_n^4 n_i^3 r_p^4 \frac{l}{I^2} + \frac{C_J}{\pi b^{3/2}} (1 + Z_{eff})^{3/2} Z_{eff} n_i^{3/2} r_p \frac{l}{I} \tag{5}$$

In the above μ= permeability k=Boltzmann Constant, Z_n=atomic number and n_i= ion number density.

3.2 Check equation (5) for the value of Pease-Braginskii current $I_{P\text{-}B}$

From (5) if we consider only the two terms, Joule heating power and the Bremsstrahlung power; then putting that version of Eqn (5) to zero we obtain the threshold current as:

$$I_{P-B}^2 = \frac{C_J}{C_1 \pi^2 b^2} \frac{(1 + Z_{eff})^2}{Z_{eff}^2} = \frac{4 C_J}{C_1 \pi^2 b^2} \tag{6}$$

Noting that for hydrogen Z_{eff}=1; and $I_{P\text{-}B}$ computes correctly to a value of 1.6 MA.

3.3 Line Radiation greatly reduces the threshold current

Considering the general case with all three power terms of Eqn (5) we obtain:

$$I^2 = \frac{C_J (1 + Z_{eff})^2}{C_1 \pi^2 b^2 Z_{eff}^2} \times \frac{C_2 Z_{eff}^2}{\left[C_2 Z_n^4 T^{-3/2} + C_1 Z_{eff}^2\right]} \tag{7}$$

So that we may write:

$$I^2 = \frac{I_{P-B}^2}{4} \times \frac{1}{\left[\frac{C_2 Z_n^4 T^{-3/2}}{C_1 Z_{eff}^2} + 1\right]} \times \frac{(1 + Z_{eff})^2}{Z_{eff}^2} \tag{8}$$

Or $$I^2 - I_{P-B}^2 \times \frac{1}{K} \quad (9)$$

Where $$K = 4\left[\frac{(dQ_{line}/dt) + (dQ_{Brem}/dt)}{(dQ_{Brem}/dt)}\right] \quad (10)$$

Note that in Eqn (8) above the factor $Z_{eff}^2 / (1+ Z_{eff})^2 \sim 1$ since Z_{eff} has the value >10 for typical plasma focus operation in Ar, Kr and Xe; and with this approximation Eqn (9) holds.

For Eqn (10) in plasma focus operation in Kr, typically in the range 100 to 1000 eV, the ratio $[dQ_{line}/dt \,/\, dQ_{Brem}/dt]$ has the range 1000 times to 10 times; so the threshold current is reduced from I_{P-B} by a factor of ~30 at 100 eV to ~3 times at 1000 eV; ie to ~50 kA at 100eV and to ~500 kA at 1000 eV. In other words at the lower temperature end of plasma focus operation in Kr a current of 50 kA may be enough to reach the threshold at which line radiation begins to exceed joule heating.

Summarising: This greatly-reduced threshold current is reflected in Eqn (9) where the reduction factor *K* is seen in Eqn (10) to be a large factor since line radiation greatly exceeds Bremsstrahlung.

3.4 Effect of plasma self-absorption

We also note that the above consideration has not taken into account the effect of plasma self-absorption. Taking that into consideration the emission power will be reduced, effectively reducing the value of *K* thus raising the threshold current from that value computed in Eqn (9).

The Lee Model code incorporates radiation-coupled dynamics [9] using the following equation:

$$\frac{dr_p}{dt} = \frac{\frac{-r_p}{\gamma I}\frac{dI}{dt} - \frac{1}{\gamma+1}\frac{r_p}{Z_f}\frac{dZ_f}{dt} + \frac{4\pi(\gamma-1)}{\mu\gamma Z_f}\frac{r_p}{f_c^2 I^2}\frac{dQ}{dt}}{\frac{\gamma-1}{\gamma}} \quad (11)$$

where *dQ/dt* is computed from Eqn (5)

Plasma self-absorption [9,43,44] is included by computing the value of plasma self-absorption correction factor A_{ab}:

$$A_{ab} = \left[(1 + 10^{-20} n_i Z_{eff})\right]^{-(1+M)} \quad (12)$$

where T_{ev} is the temperature in eV and M is the photonic excitation number:

$$M = 1.66 \times 10^{-15} r_p Z_n^{1/2} n_i / (Z_{eff} T_{eV}^{3.5}) \quad (13)$$

When there is no plasma self-absorption A_{ab} =1. When A_{ab} goes below 1, plasma self absorption starts. When a sizeable fraction of the photons is re-absorped e.g. value of A_{ab} reaches 1/e, plasma radiation is considered to switch over from volume radiation to surface radiation and is computed accordingly in the model.

Summarizing: The code computes the amount of radiation emitted, computes plasma self absorption effects and incorporates these effects into the plasma dynamics.

4 Numerical Experiment in krypton demonstrating radiative collapse

The UNU ICTP PFF [15] has the following parameters: 30 μF, 110 nH, 12 mΩ resistance, b=3.2 cm, a=0.95 cm, z_0=16 cm. We carried out numerical experiments at 12 kV krypton (model parameters taken as 0.0258, 0.7, 0.16, 0.7) at varying pressures from 0.1 -2.0 Torr. The radial trajectories are shown in Figures 2a-2f.

It is clear from Figure 2 that radiative cooling reduces the pinch radius as pressure is increased, above 0.1 Torr. Strong radiative collapse is evident in the range 0.5 to 1.6 Torr (Figs 2b-2e).

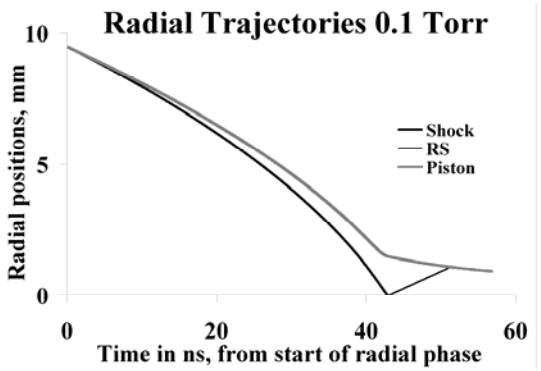

Figure 2a. Radial trajectories at Kr 0.1 Torr

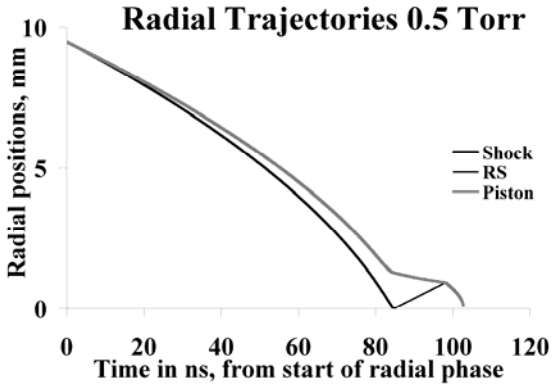

Figure 2b. Radial trajectories at Kr 0.5 Torr

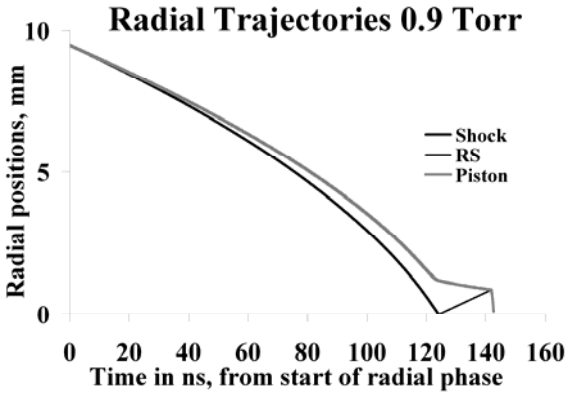

Figure 2c. Radial trajectories at Kr 0.9 Torr

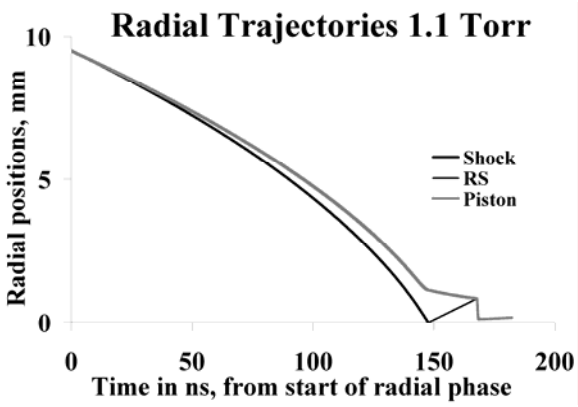

Figure 2d. Radial trajectories at Kr 1.1 Torr

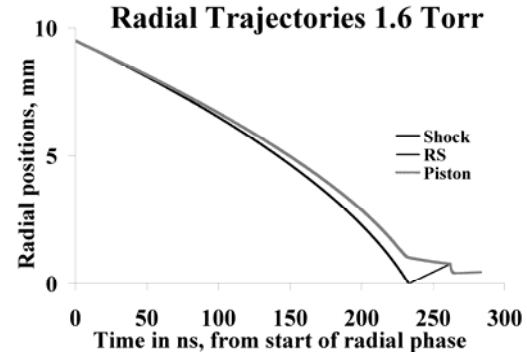

Figure 2e. Radial trajectories at Kr 1.6 Torr

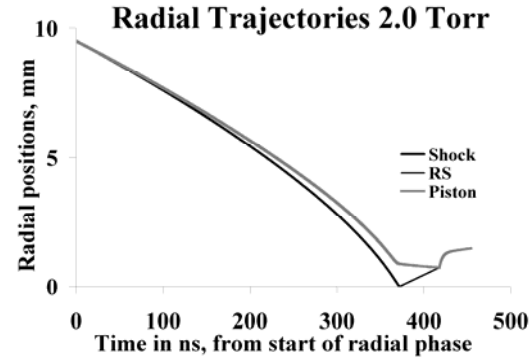

Figure 2f. Radial trajectories at Kr 2.0 Torr

Figure 2a acts as a reference situation and shows the radial dynamics at 0.1 Torr. The radial inward shock wave starts at 9.5 mm and is driven to the axis after 43 ns with the driving magnetic piston trailing it by some 1.5 mm as the shock front hits the axis. A reflected shock RS goes outwards and after some 9 ns hits the incoming piston. At this time the pinch starts and the column compresses inwards a little, as is typical. Computed data indicates that even in this shot the radiation power emitted (mostly line) already exceeds the Joule heating power with the pinch temperature in this shot reaching 1.5 keV. This means that there is already net power loss (or radiation cooling) but the radiation cooling is insufficient to perceptibly affect the dynamics at the pinching power provided by the available pinch current at that time.

At 0.5 Torr and a pinch temperature of 520 eV (see Fig 5) with a pinch current of just under 100 kA (see Fig 4), radiative collapse is obvious (see Fig 2b) with the radius collapsing in a few ns to the cut-off radius of 0.1mm set in the model. At 0.9 Torr with a pinch temperature of 300

eV and a pinching current of just 80 kA, the radiative collapse is so strong as to produce collapse to cut-off radius in less than 1 ns.

At 1.1 Torr with a pinch temperature of 220 eV, the collapse does not reach the cut-off radius. In this case the pinch maintains a small radius (0.2 mm) for 10ns. These are the conditions (high density, relatively long pinch duration) which produce huge line yields of more than 100 J. At 1.6 Torr and pinch temperature of 105 eV with a pinch current of just 57 kA, the speeds are much slower now and the pinch occurs late so the current has dropped considerably reducing the pinching force; the radiative collapsed radius is now bigger (0.6 mm). Finally at 2 Torr, the radial phase starts very late at 4.9 μs (peak circuit current is at 2.9 μs) and takes 0.4 μs to reach the pinch phase; by which time the circuit current has dropped to 50 kA way below its peak of 168 kA. There is insufficient pinching force and the column blows out instead of pinching in as the RS hits the piston.

From each of the shots (numerical experiment) shown in Fig 2 is also recorded computed data of that shot including energy distributions and plasma properties. Some of the data is collected in the following Figures. Figures 3-5 show the pinch radius, I_{peak} and I_{pinch} and pinch temperature. Other data not shown includes Z_{eff} which reduces from 30 at 0.1 Torr to 10 at 2 Torr. It is clear from Fig 3 that radiative cooling reduces the pinch radius as pressure is increased above 0.1 Torr. Strong radiative collapse is evident in the range 0.4 to 1.5 Torr with the radius dropping to the 0.01 'a' cut-off radius imposed in the model.

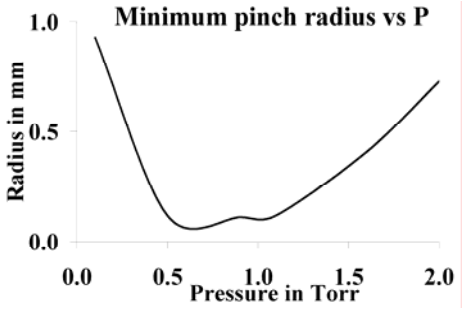

Figure 3. Minimum Pinch radius vs Pressure

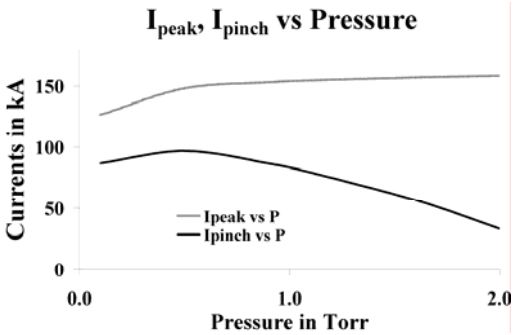

Figure 4. I_{peak}, I_{pinch} vs Pressure

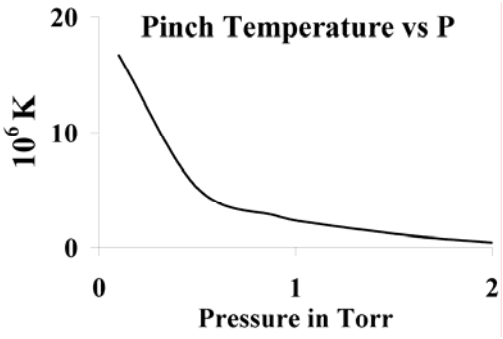

Figure 5. Pinch Temperature vs Pressure

5 Conclusion

The Lee Model code includes the effect of energy gain/loss into its dynamics, moreover incorporates the effect of plasma self-absorption. The code was run in Kr and demonstrates radiative cooling leading to radiative collapse at a pinch current ranging from 60-100 kA.

References

1 Bernard A., Bruzzone H., Choi P., Chuaqui H., Gribkov V., Herrera J., Hirano K., Krejci A., Lee S., Luo C., Mezzetti F., Sadowski M., Schmidt, H., Ware, K., Wong, C.S., Zoita, V. *Moscow J Phys Soc*, **8**(1998) 93-170.

2 Lee S., P. Lee, Zhang G., Feng X., Gribkov V. A., Liu M., Serban A., and Wong T., *IEEE Trans. Plasma Sci.*, ***26*** (1998) 1119–1126.

3 Lebert R., Neff W, Rothweiler D., J X-Ray Sci and Tech **6** (1996) 2.

4. Gribkov, V.A., Srivastava, A., Lee, P C K,. Kudryashov V. and Lee S., *IEEE Trans Plasma Sci* **30** (2002) 1331 – 1338.

5. Rishi Verma, Lee P., Lee S., Springham S V., Tan T L., Rawat R S. and Krishnan M., *Appl. Phys. Lett*. **93**, **(2008)** 101501

6. Pease, R. *Procs Phys Soc.* **70** (1957) 11.

7. Braginskii, S. *Zh Eksp Teor Fiz* **33** (1957) 645.

8. Koshelev K N., Krauz V I., Reshetniak N G., Salukvadze R G., Sidelnikov Yu V., Khautiev E Yu., *J. Phys. D: Appl. Phys.* **21** (1988)1827.

9. Lee S. Radiative Dense Plasma Focus Computation Package: RADPF. http://www.plasmafocus.net (2010)

10. Lee S. in *Radiations in Plasmas* Vol II, edited by McNamara, B. (World Scientific, Singapore) (1984) p. 978–987.

11. Tou T Y., Lee S., Kwek K H., *IEEE Trans. Plasma Sci.* **17** (1989) 311–315.

12. Lee, S. *IEEE Trans. Plasma Sci.***,** ***19*** (1991) 5

13. Lee S., Tou T Y., Moo S P., Eissa M A., Gholap A V., Kwek K H., Mulyodrono S., Smith A J., Suryadi S., Usada W., and Zakaullah M., *Amer J Phys* ***56*** (1988) 62–68.

14 Lee S. and Serban A.,. *IEEE Trans. Plasma Sci.*, ***24***. (1996). 1101–1105.

15. Jalil bin Ali, *Development and studies of a small plasma focus*, Ph.D. Dissertation; (Universiti Teknologi Malaysia, Malaysia) (1990)

16 Potter D E., *Nucl. Fusion.* ***18*** (1978) 813–823.

17. Bing S. *Plasma dynamics and X-ray emission of the plasma focus*, Ph.D. dissertation, (Nanyang Technological University, Singapore) (2000).

18. Serban A. and Lee S., *J. Plasma Phys.*, ***60*** (1998) 3–15.

19. Liu M.H., Feng X.P., Springham S V. and Lee S., *IEEE Trans. Plasma Sci.*, ***26*** (1998) 135

20. Lee S. *Twelve Years of UNU/ICTP PFF—A Review*. (Abdus Salam ICTP, Trieste) (1998). IC/ 98/ 231, p 5–34
21. Springham S. V., Lee S. and Rafique M. S., *Plasma Phys. Control. Fusion*, **42**.(2000) 1023
22. Lee S. (2010). [Online]. Available: http://ckplee.myplace.nie.edu.sg/plasmaphysics/
23. Wong D., Lee P., Zhang T., Patran A., Tan T. L., Rawat R. S., and Lee S., *Plasma Sources Sci. Technol.* ***16*** (2007) 116–123
24. Siahpoush V., Tafreshi M. A., Sobhanian S., and Khorram S., *Plasma Phys. Control. Fusion*, ***47*** (2005) 1065–1075.
25. Lee S. and Saw S. H., *J. Fusion Energy*, ***27*** (2008) 292–295.
26 Lee S., *Plasma Phys. Control. Fusion*, ***50*** (2008) 105 005
27. Lee S., Saw S. H., Lee P. C. K., Rawat R.S., and Schmidt H., *Appl. Phys. Lett.*, ***92*** (2008) 111 501.
28. Lee S. and Saw S. H., *Appl. Phys. Lett.*, ***92*** (2008) 021 503.
29. Lee S., Lee P., Saw S. H., and Rawat R. S., Plasma Phys. Control. Fusion **50** (2008) 065012
30. Lee S., *Appl Phys Lett*, ***95*** (2009) 151503
32. Lee S., Saw S. H., Soto L., Moo S. P., Springham S. V., *Plasma Phys. Control. Fusion*, ***51*** (2009) 075006
33. Lee S., Saw S. H., Lee P. & Rawat R. S., *Plasma Physics and Controlled Fusion*, ***51*** (2009) 105013
34. Akel M, Al-Hawat Sh., Saw S H. and Lee S., *J Fusion Energy* , **29** (2010) 223–231
35. Lee S., Rawat R. S., Lee P., Saw S. H., *J Appl Phys*, ***106*** (2009) 023309.
36. Saw S. H., Lee P. C. K., Rawat R. S. and Lee S. *IEEE Trans Plasma Sc*, ***37*** (2009) 1276
37. Chow S. P., Lee S.,and Tan B. C., *J. Plasma Phys*., 8 (1973) 21-31.
38. Favre M., Lee S., Moo S. P., Wong C. S., *Plasma Sources Sci and Tech*, **1** (1992) 122
39. McWhirter in "Plasma Diagnostic Techniques" edited by Huddelstone, R H and Leonard S L (Academic Press, New York) (1965)
40. http://physics.nist.gov/PhysRefData/Elements/
41. Lee S., *Australian J Phys* **35** (1983) 391.
42. Koshelev K. and Pereira N., *J Appl. Phys*. **69** (1991) 21-44
43 Robson, A E., *Phys. Fluid B3* (1991) 1481
44 Khattak, N A D. Anomalous Heating (LHDI). http://www.plasmafocus.net/IPFS/modelpackage/File3Appendix.pdf (2011)